



Universiteit
Leiden
The Netherlands

Steering the selectivity of electrocatalytic glucose oxidation by the Pt oxidation state

Ham, M.P.J.M. van der.; Keulen, E. van; Koper, M.T.M.; Tashvigh, A.A.; Bitter, J.H.

Citation

Ham, M. P. J. M. van der., Keulen, E. van, Koper, M. T. M., Tashvigh, A. A., & Bitter, J. H. (2023). Steering the selectivity of electrocatalytic glucose oxidation by the Pt oxidation state. *Angewandte Chemie (International Edition)*, 62(33). doi:10.1002/anie.202306701

Version: Publisher's Version

License: [Creative Commons CC BY 4.0 license](https://creativecommons.org/licenses/by/4.0/)

Downloaded from: <https://hdl.handle.net/1887/3716365>

Note: To cite this publication please use the final published version (if applicable).

Electrocatalytic Oxidation

Steering the Selectivity of Electrocatalytic Glucose Oxidation by the Pt Oxidation State

Matthijs P. J. M. van der Ham, Ellis van Keulen, Marc T. M. Koper, Akbar Asadi Tashvigh, and Johannes H. Bitter*

Abstract: Electrocatalytic glucose oxidation can produce high value chemicals, but selectivity needs to be improved. Here we elucidate the role of the Pt oxidation state on the activity and selectivity of electrocatalytic oxidation of glucose with a new analytical approach, using high-pressure liquid chromatography and high-pressure anion exchange chromatography. It was found that the type of oxidation, i.e. dehydrogenation of primary and secondary alcohol groups or oxygen transfer to aldehyde groups, strongly depends on the Pt oxidation state. Pt⁰ has a 7-fold higher activity for dehydrogenation reactions than for oxidation reactions, while PtO_x is equally active for both reactions. Thus, Pt⁰ promotes glucose dialdehyde formation, while PtO_x favors gluconate formation. The successive dehydrogenation of gluconate is achieved selectively at the primary alcohol group by Pt⁰, while PtO_x also promotes the dehydrogenation of secondary alcohol groups, resulting in more complex reaction mixtures.

Glucose is a widely abundant biomass-based feedstock, that can be electrocatalytically oxidized by (or cogenerate) renewable electricity to yield numerous chemicals that are of great interest in the chemical industry.^[1] The most relevant products are glucaric acid and gluconic acid, which are among the top value-added chemicals mentioned by the National Renewable Energy Laboratory.^[1b,2] Other glucose oxidation products include 2-keto gluconic acid,^[3] 5-keto gluconic acid,^[4] and glucuronic acid.^[5] These glucose oxidation products are (precursors to) platform molecules and specialty chemicals that are used as building blocks or as additives in pharmaceuticals, food, feed, and materials.^[1b,2-6]

However, currently the mechanism behind the catalyst selectivity for the (electro-)oxidation of glucose and how to steer it to a desired product is not yet fully understood. To steer the selectivity it is essential to understand the reaction pathway, which requires the quantification of all (intermediate) products during the glucose oxidation reaction. Several chemocatalytic^[7] and electrocatalytic^[3,8] studies have investigated the glucose oxidation pathway, where different analytical techniques (e.g., 2D NMR,^[7a] HPIC,^[7c,8b] and HPLC,^[3,7b,c,8a] HPLC-MS,^[7b] and GC-MS^[3]) have been applied in an attempt to quantify the (intermediate) glucose oxidation products. Still, various (intermediate) products have not been addressed even though they are expected to be formed during the reaction. Some examples include glucose dialdehyde (only mentioned, but never quantified),^[3,7,8] guluronic acid or glucuronic acid (often only one or the other is quantified),^[3,7b-d,8] and 2-keto gluconic acid and 5-keto gluconic acid (seldomly quantified).^[7a,b,8a]

The similarity in the structures of glucose oxidation products poses a challenge in their differentiation and may result in inadequate separation by the analytical technique employed. This problem in correctly identifying glucose oxidation products can be observed for guluronic acid and glucuronic acid, which are stereoisomers.^[7a] As a result, it has been claimed that gluconic acid can be oxidized to glucuronic acid,^[3,7c] while guluronic acid is expected based on the stereochemistry of the molecules. Moreover, for an adequate separation of guluronic acid and glucuronic acid, other techniques than HPLC or GC are required, as has been shown for the compositional analysis of seaweed (e.g., consisting of guluronic acid and glucuronic acid).^[9]

Here, we address this challenge by introducing a new analytical approach that combines high-pressure liquid chromatography (HPLC)^[10] with high-pressure anion exchange chromatography (HPAEC).^[9] Unlike other analytical techniques, HPAEC separates ionizable molecules based on their total charge. This analytical approach enables us to quantify all (intermediate) products in the glucose oxidation pathway, allowing us to 1) simultaneously quantify guluronic acid, glucuronic acid, 2-keto gluconic acid, and 5-keto gluconic acid and 2) quantify glucose dialdehyde. With this analytical approach in hand, we can draw a complete map of the reaction pathway for the electrocatalytic oxidation of glucose and show how in detail the Pt oxidation state affects the selectivity.

Figure 1A shows the linear sweep voltammograms (LSV) of glucose oxidation and of the oxidation of the main glucose oxidation products (gluconate and glucuronate) on a

[*] M. P. J. M. van der Ham, E. van Keulen, Dr. A. A. Tashvigh, Prof. Dr. J. H. Bitter
 Biobased Chemistry and Technology, Wageningen University & Research
 P.O. Box 17, 6700 AA Wageningen (The Netherlands)
 E-mail: harry.bitter@wur.nl

M. P. J. M. van der Ham, Prof. Dr. M. T. M. Koper
 Catalysis and Surface Chemistry, Leiden University
 P.O. Box 9502, 2300 RA Leiden (The Netherlands)

© 2023 The Authors. Angewandte Chemie International Edition published by Wiley-VCH GmbH. This is an open access article under the terms of the Creative Commons Attribution License, which permits use, distribution and reproduction in any medium, provided the original work is properly cited.

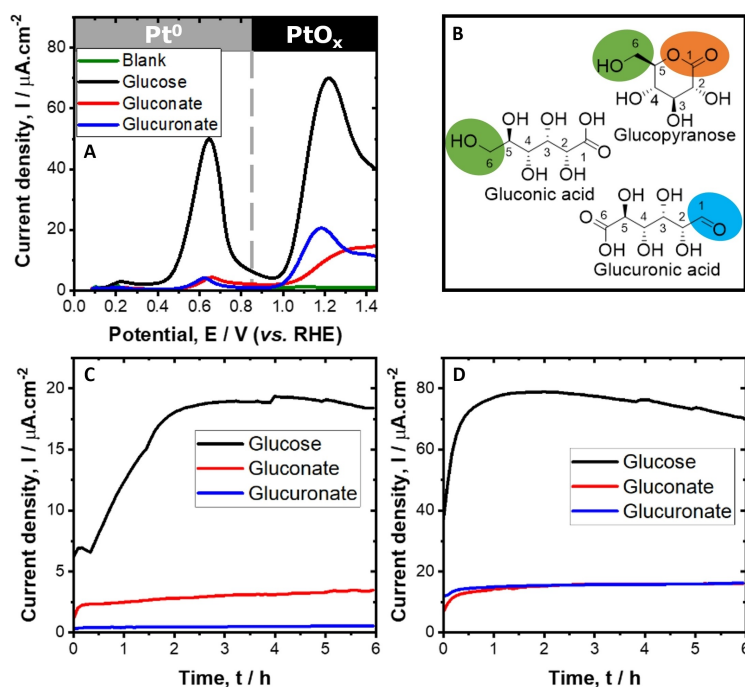


Figure 1. Blank LSV and LSV of 0.1 M glucose, 0.1 M gluconate, and 0.1 M glucuronate in 0.2 M PBS (pH = 7) on a polycrystalline Pt electrode recorded at a scan rate of 1 mV s^{-1} . The potential windows 0–0.85 V and > 0.85 V vs. RHE correspond to Pt^0 and PtO_x , respectively. B) The dominant structures of glucose (e.g., glucopyranose), gluconate and glucuronate at the studied reaction conditions (for simplicity the structures have been drawn in protonated form) in which the main reactive groups are highlighted. Current-time curves for the electrocatalytic oxidation of 0.1 M glucose, 0.1 M gluconate, and 0.1 M glucuronate in 0.2 M PBS over Pt^0 (0.64 V vs. RHE, C) and PtO_x (1.2 V vs. RHE, D).

polycrystalline Pt electrode in a pH = 7 buffer solution (0.2 M phosphate buffer solution, PBS). These reaction conditions were chosen to avoid non-electrochemical side reactions, such as isomerization, retro-aldol and aldol condensation reactions.^[11] 0.1 M reactant concentrations were used to avoid the overload of the detectors of the chromatographic equipment and to prevent high conversions of the reactants. This all enables the discrimination between catalytic activities towards different reactants. Figure 1B displays the dominant structures of glucose,^[12] gluconate,^[13] and glucuronate^[14] under the studied reaction conditions and highlights the most reactive groups of these species.

For glucose oxidation, Figure 1A shows two oxidation peaks, at 0.64 V and 1.2 V vs. RHE respectively.^[15] This characteristic LSV is common for the electrochemical oxidation of small organic molecules, indicating the presence of two reaction pathways for oxidation.^[15,16] Since the first anodic peak is below the Pt surface oxidation potential, Pt is expected to be mainly in its metallic state (Pt^0 , though steps and defects sites are likely mildly oxidized^[17]), while the second anodic peak is above the surface oxidation potential of Pt and hence the surface is in a more oxidized state (referred to as PtO_x).^[16a,18] Figure S1 shows the CV of Pt in 0.2 M PBS to give a better understanding of its surface structure and its oxidation state as a function of the applied potential. The LSV of glucose shows a peak potential at 0.64 V vs. RHE, corresponding well to the LSV of Pt(110)-type sites.^[19] For Pt^0 , an anodic current density of ca. $50 \mu\text{A cm}^{-2}$ can be observed for the electrocatalytic oxida-

tion of glucose, while a much lower current density is observed for gluconate and glucuronate oxidation ($4 \mu\text{A cm}^{-2}$). PtO_x shows an anodic current density for the electrocatalytic oxidation of glucose of ca. $70 \mu\text{A cm}^{-2}$ and also a lower anodic current density for gluconate ($10 \mu\text{A cm}^{-2}$) and glucuronate ($20 \mu\text{A cm}^{-2}$) oxidation, but the difference is less pronounced than on Pt^0 .^[20] This indicates that the catalytic activity of Pt^0 follows glucose \gg gluconate \sim glucuronate, while the activity of PtO_x follows glucose $>$ glucuronate $>$ gluconate.

For chronoamperometric measurements, the applied reaction conditions were optimized to limit mass transport limitations by applying convection (Figure S2), to retain a constant pH by buffering with 0.2 M PBS (Figure S3), and to retain an active catalyst by applying a potential program (Figure S3).^[8b,20]

Figures 1C and 1D show the chronoamperometric measurements for the electrocatalytic oxidation of glucose, gluconate, and glucuronate on Pt^0 (0.64 V vs. RHE) and PtO_x (1.2 V vs. RHE), respectively. The current densities do not significantly change from 2 to 6 h, indicating that the formation of (intermediate) products do not significantly affect the catalyst activity. After 6 h of reaction on Pt^0 (0.64 V vs. RHE), the current density for the electrocatalytic oxidation of glucose ($18 \mu\text{A cm}^{-2}$) is a 5-fold higher than for gluconate ($3.5 \mu\text{A cm}^{-2}$) and a 12-fold higher than for glucuronate ($0.5 \mu\text{A cm}^{-2}$). By contrast, after 6 h of oxidation on PtO_x (1.2 V vs. RHE), the current densities for the electrocatalytic oxidation of glucose ($70 \mu\text{A cm}^{-2}$) is a 4-fold

higher than for gluconate and glucuronate ($16 \mu\text{A cm}^{-2}$ each). The overall lower catalytic activity of Pt^0 compared to PtO_x can be attributed to the lower applied potential for Pt^0 and a partial CO poisoning of Pt^0 .^[19,21] These results indicate that both Pt^0 and PtO_x exhibit higher catalytic activity in the oxidation of glucose as compared to gluconate or glucuronate oxidation. By contrast, PtO_x is equally active for catalyzing the oxidation of gluconate and glucuronate, while Pt^0 is more active for catalyzing the oxidation of gluconate than glucuronate. This shows that Pt^0 is more active for catalyzing the dehydrogenation of C6–OH of gluconate than for catalyzing the oxidation of C1=O of glucuronate, while PtO_x is equally active for both reactions.^[16b,22] Moreover, this reveals that PtO_x is more active than Pt^0 for catalyzing oxygen transfer reactions. These results are in agreement with results of the electrocatalytic oxidation of methanol and glycerol.^[16b,21b,22,23] Those studies showed that Pt–Pt pair sites stabilize and dehydrogenate primary alcohols and Pt–OH sites are required for oxygen transfer reactions.^[21b,23]

All (intermediate) products formed by the electrocatalytic oxidation of glucose were quantified to establish the reaction pathway and product selectivity as a function of Pt oxidation state. Here we have developed a new analytical approach, in which High Pressure Anion Exchange Chromatography-Pulsed Amperometric Detection (HPAEC-PAD, Figure S5A–B) and High Pressure Liquid Chromatography-Refractive Index-Ultraviolet (HPLC-RI-UV, Figure S6A–B) were combined, to separate the different intermediates and products (e.g., glucose dialdehyde, gluconate, glucuronate 2-keto gluconate, 5-keto gluconate, and glucarate), enabling their quantification. The carbon balance was close to 100 % for the electrocatalytic oxidation of glucose over Pt^0 and PtO_x , indicating that all products were accurately quantified.

Figure 2A–F shows the concentrations of products as a function of time during the electrocatalytic oxidation of glucose over Pt^0 and PtO_x , evidencing a significant effect of the Pt oxidation state on the selectivity for catalyzing different functional groups.

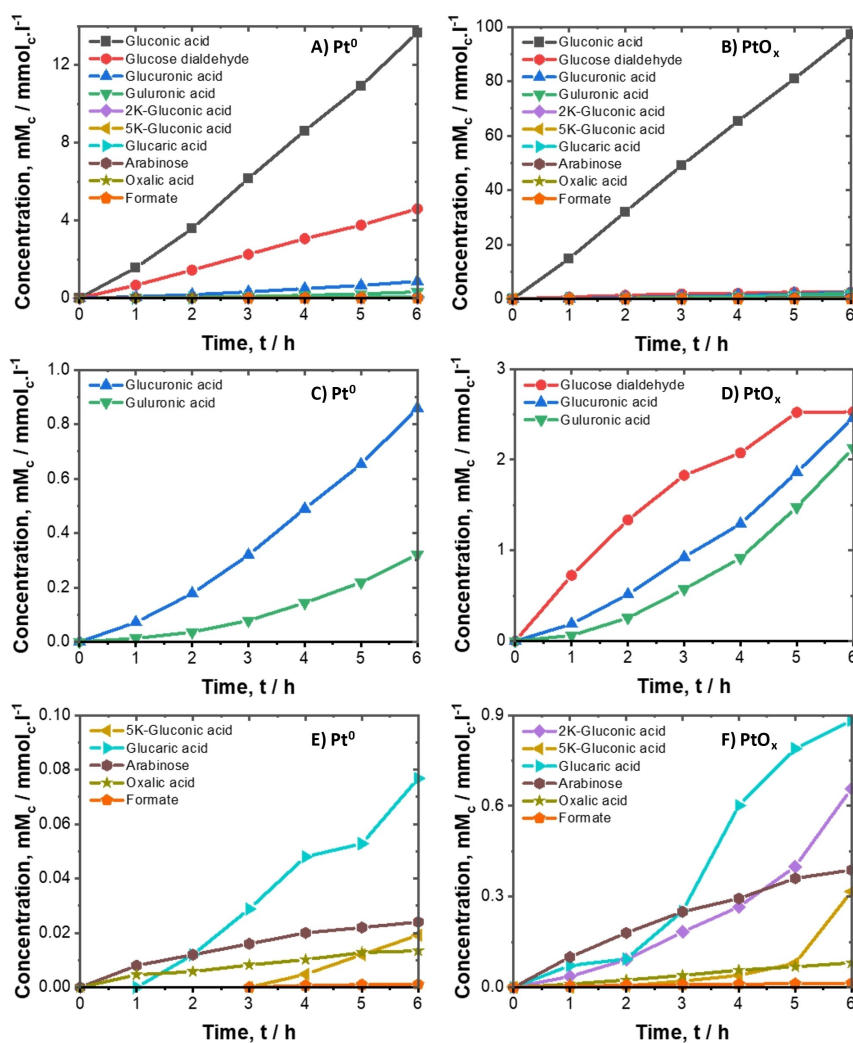


Figure 2. Major (A–B), secondary (C–D) and minor (E–F) product concentration-time curves for the electrocatalytic oxidation of glucose on Pt^0 and PtO_x in 0.2 M PBS (pH = 7).

For glucose oxidation over Pt⁰, Figure 2A shows a linear increase in gluconate and glucose dialdehyde concentration over time. This suggests that these products are formed at a constant rate, exhibiting an approximately zero-order kinetics, reaching concentrations of 13.5 and 4.6 mmol CL⁻¹ respectively. By contrast, PtO_x (Figure 2B) is much more active for gluconate production (reaching 98 mmol CL⁻¹), while the production of glucose dialdehyde (Figure 2D) only reaches 2.5 mmol CL⁻¹. This reveals that Pt⁰ is more active towards the electrocatalytic dehydrogenation of the C6–OH of glucose, while PtO_x favors the electrocatalytic dehydrogenation/oxidation of glucose, in line with the electrocatalytic oxidation of methanol and glycerol over Pt⁰ and PtO_x.^[21b,23]

As for the secondary products, Figure 2C shows that the electrocatalytic oxidation of glucose on Pt⁰ results in a faster exponential increase in glucuronate concentration compared to guluronate concentration. For PtO_x, Figure 2D reveals that the exponential increase in glucuronate and guluronate concentration proceed at a similar rate. The observed exponential increase in concentration suggests that guluronate and glucuronate are formed according to first-order kinetics, originating from gluconate/gluconate dialdehyde and glucose dialdehyde respectively. As a result, the higher selectivity of Pt⁰ towards glucuronate can be related to the higher selectivity towards glucose dialdehyde of Pt⁰ compared to PtO_x.

In Figure 2E and F we illustrate the formation rates of other minor products. The electrocatalytic oxidation of glucose on Pt⁰ shows an increase in 5-keto gluconate concentration (Figure 2E), while for PtO_x (Figure 2F) an increase in 2-keto gluconate and 5-keto gluconate concentration is observed. To observe these products, the application of a desorption potential (2 V vs RHE) was needed. That desorption potential also reactivated the catalyst (Figure S3). To evaluate whether these products are indeed formed during normal operation on Pt⁰ (0.64 V vs. RHE) and PtO_x (1.2 V vs. RHE) and not at the desorption potential (2.0 V vs. RHE), the theoretical coulombs required to form these products were compared to the coulombs measured at the desorption potential (all values are given in

Table S2). From these results, it is clear that PtO_x forms 2-keto gluconate and 5-keto, but it is uncertain whether Pt⁰ forms 5-keto gluconate. This implies that PtO_x is more active for the dehydrogenation of the secondary alcohol groups of gluconate, which is similar to the dehydrogenation of glycerol to dihydroxyacetone under neutral conditions^[16b] or sorbitol to fructose under acidic conditions.^[24]

The concentration profiles of glucarate over Pt⁰ and PtO_x as shown in Figure 2E–F suggest that its formation involves multiple pathways. Specifically, glucarate can be formed through the electrocatalytic oxidation of both guluronate and glucuronate. Finally, the concentration profiles of arabinose, oxalate and formate (e.g., C₅–C₁ products) over Pt⁰ and PtO_x increase gradually over time, revealing that C–C cleavage reactions are being catalyzed, but only at very low rates.

Table 1 summarizes the selectivity of the products, faradaic efficiency (FE), and turnover frequency (TOF) for the electrocatalytic oxidation of glucose, gluconate, and glucuronate on Pt⁰ and PtO_x.

The low conversions of gluconate and glucuronate during electrocatalytic oxidation made it difficult to accurately determine the carbon balance closure for these reactions. Therefore, in Table 1 the product selectivities are based on the products formed (CO and CO₂/HCO₃⁻ cannot be detected by the chromatographic techniques). However, the FE is close to 100% for all reactions and therefore shows that all products formed during CA were quantified, except for the electrocatalytic oxidation of glucuronate on Pt⁰, likely due to the low concentrations of glucarate.

The TOF for the electrocatalytic oxidation of glucose, gluconate, and glucuronate on Pt⁰ (0.64 V vs. RHE) are 0.036, 0.006 and 0.001 s⁻¹ and on PtO_x (1.2 V vs. RHE) are 2.1, 0.36 and 0.040 s⁻¹. PtO_x has a similar TOF for the electrocatalytic oxidation of gluconate and glucuronate, while Pt⁰ has a lower activity for the electrocatalytic oxidation of glucuronate. This reveals that PtO_x is equally active for catalyzing the dehydrogenation of C₆–OH of gluconate as it is for oxidation of C₁=O of glucuronate, while Pt⁰ is more active for catalyzing the dehydrogenation of

Table 1: Faradaic efficiency, TOF and product selectivity, for the electrocatalytic oxidation of 0.1 M glucose, gluconate, and glucuronate in 0.2 M PBS (pH = 7) on Pt⁰ and PtO_x. A color code was added to guide the eye, going from high (green) to low (red) selectivities. The description of the abbreviations of the (intermediate) products are given in the footnote.

Reactant	Catalyst	FE %	TOF (10 ⁻³ s ⁻¹)	Product selectivities (%) ^a							
				GA	GD	GUL	GLU	2-kGA	5-kGA	GAR	C ₅ -C ₁
Glucose	Pt ⁰	105	36	70	23	2	4	-	0.1	0.4	0.2
GA	Pt ⁰	101	6	-	-	86	-	-	3	10	1
GLU	Pt ⁰	141	1	-	-	-	-	-	-	98	2
Glucose	PtO _x	105	210	91	2	2	2	0.6	0.3	0.8	0
GA	PtO _x	114	36	-	-	70	-	12	6	9	2
GLU	PtO _x	101	40	-	-	-	-	-	-	100	0

^a GA = gluconate, GD = glucose dialdehyde, GUL = guluronate, GLU = glucuronate, 2-kGA = 2-keto gluconate, 5-kGA = 5-keto gluconate, GAR = glucarate, AR = arabinose, OA = oxalate, FA = formate

C_6 -OH of gluconate than it is for oxidation of $C_1=O$ of gluconate (Figure 1C).

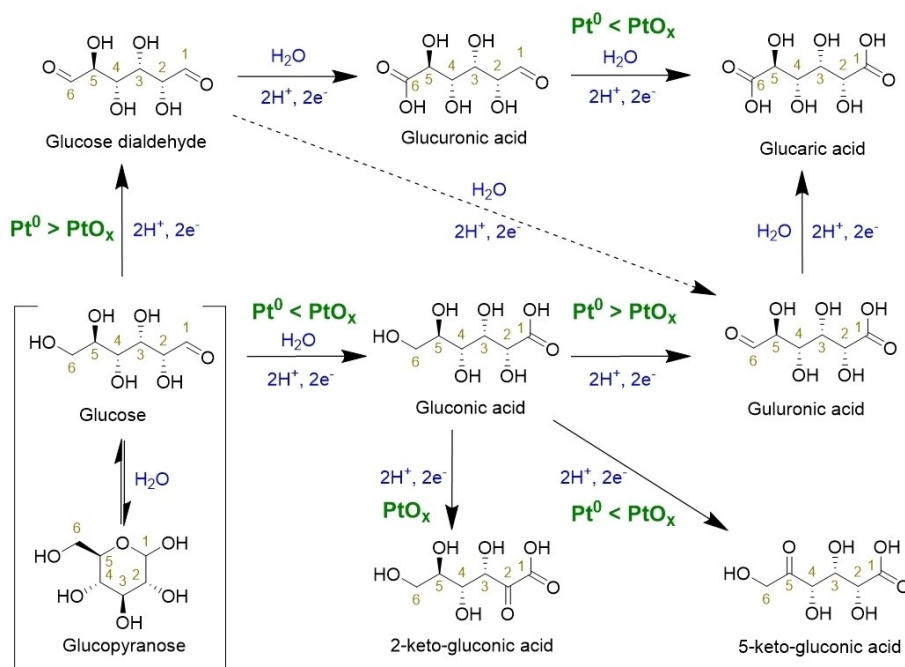
As shown in Table 1, glucose is more selectively converted to glucose dialdehyde by Pt^0 (23 %) than by PtO_x (2 %), suggesting that Pt^0 favors the dehydrogenation of C_6 -OH of glucose. By contrast, PtO_x is more selective towards gluconate (91 %), indicating that it promotes the dehydrogenation/oxidation of the anomeric carbon of glucose. In line with these results, gluconate was selectively converted to gulurionate (86 %) by Pt^0 , which shows the high selectivity of Pt^0 towards C_6 -OH dehydrogenation. By contrast, PtO_x also promotes the formation of 2-keto gluconate (12 %) and 5-keto gluconate (6 %), revealing that PtO_x also promotes secondary alcohol dehydrogenation, resulting in a loss in selectivity towards gluconate. Finally, gluconate can be converted with similar selectivity towards glucarate (~100 %) by Pt^0 and PtO_x , indicative that they both are highly selective for the electrocatalytic oxidation of $C_1=O$ of gluconate.

Scheme 1 illustrates the electrocatalytic oxidation pathways of glucose over Pt in neutral reaction conditions. It is expected that gluconate and glucose dialdehyde are primary products, while gulurionate and gluconate are secondary products. To verify this, an experiment was conducted with different initial glucose concentrations (Figure S7). This experiment revealed that a reduction in initial glucose concentration corresponds with decreased selectivity towards primary oxidation products (gluconate and glucose dialdehyde) and an increase in selectivity towards secondary oxidation products (gulurionate and gluconate).

The scheme also highlights the preferred pathways for Pt^0 and PtO_x . Firstly, glucose can either be dehydrogenated

at the C_6 -OH to glucose dialdehyde or dehydrogenated/oxidized at the anomeric carbon to gluconate. In this case, Pt^0 promotes the dehydrogenation of C_6 -OH of glucose and therefore drives the selectivity towards glucose dialdehyde. By contrast, PtO_x can promote both dehydrogenation and oxidation (e.g., oxygen transfer) reactions and therefore favors the dehydrogenation/oxidation of the anomeric carbon of glucose, resulting in a high selectivity towards gluconate. Secondly, gluconate can either be dehydrogenated at the primary alcohol group (C_6 -OH) to gulurionate or at the secondary alcohol group (C_2 -OH and C_5 -OH) to 2-keto gluconate and 5-keto gluconate. Pt^0 promotes the dehydrogenation of C_6 -OH of gluconate and might have some activity for the dehydrogenation of the C_5 -OH, resulting in minor contents of 5-keto gluconate. In addition, PtO_x can dehydrogenate both the primary and secondary alcohol groups of gluconate, resulting in a complex mixture of products containing amongst others gulurionate, 2-keto gluconate, and 5-keto gluconate. Finally, gluconate can be oxidized at $C_1=O$ to glucarate. Both Pt^0 and PtO_x are selective for this reaction. Yet, PtO_x has a considerably higher activity for this reaction than Pt^0 , which indicates that Pt needs to be oxidized to promote oxidation/oxygen-transfer reactions under neutral conditions.

In conclusion, we have developed a new analytical approach to identify and quantify all glucose oxidation products and investigate the influence of Pt oxidation state on the selectivity and activity of the catalyst for the electrocatalytic oxidation of glucose. We found that Pt^0 is more active for primary alcohol dehydrogenation than aldehyde oxidation, promoting the formation of glucose dialdehyde from glucose and gulurionate from gluconate. Hence, Pt^0



Scheme 1. Reaction pathways for the electrocatalytic oxidation of glucose on Pt^0 and PtO_x in neutral solution (for simplicity the structures have been drawn in protonated form).

drives the selectivity towards the dehydrogenation of primary alcohol groups at the expense of aldehyde oxidation reactions and anomeric carbon dehydrogenation/oxidation. On the other hand, PtO_x is equally active for catalyzing aldehyde oxidation and primary alcohol dehydrogenation, thereby promoting the formation of gluconate from glucose and glucarate from glucuronate. Hence, PtO_x increases the selectivity towards the electrocatalytic dehydrogenation/oxidation of the anomeric carbon at the expense of primary alcohol dehydrogenation. Despite the high selectivity of PtO_x towards gluconate, it also promotes its successive dehydrogenation of secondary alcohol groups, leading to complex reaction mixtures. This role of the Pt oxidation state on the catalyst selectivity and activity for the electrocatalytic oxidation of glucose illustrates how the catalyst properties can crucially affect product distribution.

Acknowledgements

This work is partially financed by the Dutch Research Council (NWO) and is part of the research program Electrons to Chemical Bonds (E2CB) with project number P17-08-05.

Conflict of Interest

The authors declare no conflict of interest.

Data Availability Statement

The data that support the findings of this study are available from the corresponding author upon reasonable request.

Keywords: Chromatography · Dehydrogenation · Electrocatalytic Oxidation · Glucose · Pt Oxidation State

- [1] a) K. Xie, A. Ozden, R. K. Miao, Y. Li, D. Sinton, E. H. Sargent, *Nat. Commun.* **2022**, *13*, 3070; b) T. Werpy, G. Petersen, *Top Value Added Chemicals from Biomass: Volume I—Results of Screening for Potential Candidates from Sugars and Synthesis Gas*, **2004**.
- [2] Y. Li, X. Wei, L. Chen, J. Shi, *Angew. Chem. Int. Ed.* **2021**, *60*, 19550–19571.
- [3] K. B. Kokoh, P. Parpot, E. M. Belgsir, J. M. Léger, B. Beden, C. Lamy, *Electrochim. Acta* **1993**, *38*, 1359–1365.
- [4] Z. Luo, S. Yu, W. Zeng, J. Zhou, *Biotechnol. Adv.* **2021**, *47*, 107706.
- [5] P. N. Amaniampong, A. Karam, Q. T. Trinh, K. Xu, H. Hirao, F. Jérôme, G. Chatel, *Sci. Rep.* **2017**, *7*, 1–8.
- [6] a) W. Deng, L. Yan, B. Wang, Q. Zhang, H. Song, S. Wang, Q. Zhang, Y. Wang, *Angew. Chem. Int. Ed.* **2021**, *60*, 4712–4719; b) J. N. Chheda, G. W. Huber, J. A. Dumesic, *Angew. Chem. Int. Ed.* **2007**, *46*, 7164–7183; c) T. Ishida, M. Haruta, *Angew. Chem. Int. Ed.* **2007**, *46*, 7154–7156.
- [7] a) R. D. Armstrong, J. Hirayama, D. W. Knight, G. J. Hutchings, *ACS Catal.* **2019**, *9*, 325–335; b) J. Lee, B. Saha, D. G. Vlachos, *Green Chem.* **2016**, *18*, 3815–3822; c) X. Jin, M. Zhao, M. Vora, J. Shen, C. Zeng, W. Yan, P. S. Thapa, B. Subramaniam, R. V. Chaudhari, *Ind. Eng. Chem. Res.* **2016**, *55*, 2932–2945; d) E. Derrien, P. Marion, C. Pinel, M. Besson, *Org. Process Res. Dev.* **2016**, *20*, 1265–1275.
- [8] a) W. J. Liu, Z. Xu, D. Zhao, X. Q. Pan, H. C. Li, X. Hu, Z. Y. Fan, W. K. Wang, G. H. Zhao, S. Jin, G. W. Huber, H. Q. Yu, *Nat. Commun.* **2020**, *11*, 265; b) K. B. Kokoh, J. M. Léger, B. Beden, H. Huser, C. Lamy, *Electrochim. Acta* **1992**, *37*, 1909–1918.
- [9] W. Huijgen, E. Cobussen-Pool, B. van Egmond, J. van Hal, *Protocols for Macroalgae Research*, Taylor & Francis, New York, **2018**, pp. 200–210.
- [10] a) Y. Wan, L. Zhang, Y. Chen, J. Lin, W. Hu, S. Wang, J. Lin, S. Wan, Y. Wang, *Green Chem.* **2019**, *21*, 6318–6325; b) S. Solmi, C. Morreale, F. Ospitali, S. Agnoli, F. Cavani, *ChemCatChem* **2017**, *9*, 2797–2806.
- [11] G. Moggia, J. Schalck, N. Daems, T. Breugelmans, *Electrochim. Acta* **2021**, *374*, 137852.
- [12] F. Largeaud, K. B. Kokoh, B. Beden, C. Lamy, *J. Electroanal. Chem.* **1995**, *397*, 261–269.
- [13] J. P. Van Dijken, A. Van Tuijl, M. A. H. Luttkik, W. J. Middelhoven, J. T. Pronk, *J. Bacteriol.* **2002**, *184*, 672–678.
- [14] R. Dowben, *Biochim. Biophys. Acta* **1959**, *31*, 454–458.
- [15] K. B. Kokoh, J. M. Léger, B. Beden, C. Lamy, *Electrochim. Acta* **1992**, *37*, 1333–1342.
- [16] a) N.-H. Li, S.-G. Sun, S.-P. Chen, *J. Electroanal. Chem.* **1997**, *430*, 57–67; b) Y. Kwon, K. J. P. Schouten, M. T. M. Koper, *ChemCatChem* **2011**, *3*, 1176–1185; c) L. Xin, Z. Zhang, J. Qi, D. Chadderdon, W. Li, *Appl. Catal. B* **2012**, *125*, 85–94.
- [17] X. Chen, I. T. McCrum, K. A. Schwarz, M. J. Janik, M. T. M. Koper, *Angew. Chem. Int. Ed.* **2017**, *56*, 15025–15029.
- [18] H. Imai, K. Izumi, M. Matsumoto, Y. Kubo, K. Kato, Y. Imai, *J. Am. Chem. Soc.* **2009**, *131*, 6293–6300.
- [19] G. A. B. Mello, W. Cheuquepán, J. M. Feliu, *J. Electroanal. Chem.* **2020**, *878*, 114549.
- [20] G. Moggia, T. Kenis, N. Daems, T. Breugelmans, *ChemElectroChem* **2020**, *7*, 86–95.
- [21] a) M. J. S. Farias, J. M. Feliu, *Top. Curr. Chem.* **2019**, *377*, 79–103; b) K. Kunimatsu, H. Hanawa, H. Uchida, M. Watanabe, *J. Electroanal. Chem.* **2009**, *632*, 109–119.
- [22] Y. Kwon, Y. Birdja, I. Spanos, P. Rodriguez, M. T. M. Koper, *ACS Catal.* **2012**, *2*, 759–764.
- [23] H. Nonaka, Y. Matsumura, *J. Electroanal. Chem.* **2002**, *520*, 101–110.
- [24] Y. Kwon, E. De Jong, J. K. Van Der Waal, M. T. M. Koper, *ChemSusChem* **2015**, *8*, 970–973.

Manuscript received: May 12, 2023

Accepted manuscript online: June 24, 2023

Version of record online: July 4, 2023